The effect of variable cloud micro- and macrophysical properties on the solar radiative transfer in the cloudy atmosphere

Cumulative Habilitation Thesis

Dr. Andreas Macke

Kiel
2001

Contents

1 Introduction

Clouds are an impressive manifestation of complex dynamical-thermodynamical processes in the atmosphere (see Fig. 1). They influence our weather and climate and are affected by anthropogenic climate changes at the same time.

With a global coverage of more than 60 % clouds have a prevailing effect on the radiation budget of our planet. Latent heat from condensation processes helps driving atmospheric circulation cells, which in turn interact with the ocean system (e.g. ENSO). (Negative) latent heat is transported by cloud related condensation and evaporation processes, and the corresponding transports of fresh water determine vegetation over land and the stability of the oceanic boundary layer.

This well recognized significance of the cloudy atmosphere on the state of the earth's climate stands in strong contrast to our quantitative understanding of the relevant physical processes in clouds. The reasons for this are 1) the complex macro- and microphysical properties of clouds, 2) their fast temporal development, and 3) their difficult experimental accessibility.

For example, it is well known that the cloud albedo effect dominates the cloud greenhouse effect, thus clouds are cooling our climate system (Wielicki et al., 1995). However, estimations of the global mean value of this so-called net radiative forcing range from -18 to -30 Wm^{-2} (Ramanathan et al., 1989; Rossow, 1993) depending on the method and time of observation. The uncertainties are much larger at local scales and for specific cloud types.

For many years a potential discrepancy between theoretically expected and observationally derived solar broadband cloud absorption termed 'anomalous cloud absorption' ranging from 15 to 35 Wm^{-2} has been discussed (Fritz and MacDonald, 1951; Cess and co authors, 1995; Ramanathan and co authors, 1995). However, since the absorbed solar flux can only be obtained indirectly from balancing measurements of reflected and transmitted solar radiation, and because those measurements are subject to large statistical errors, the cloud anomalous absorption is subject to much debate (Stephens and Tsay, 1990). On the other hand, the simplified treatment of cloud radiative transfer in climate models may explain the discrepancies as well (Cairns et al., 2000).

According to the IPCC report "Climate Change 2001" the increase of CO_2 from 1750 until today produces with +1.4 Wm^{-2} the largest anthropogenically induced change in the global radiative forcing. Comparing this number with the uncertainties of about 20 Wm^{-2} in cloud radiative forcing clearly demonstrates that a reasonable exploration and prediction of our climate system requires a much improved understanding of cloud-radiation interactions.

The aim of the work summarized in this thesis is to account for most realistic cloud properties in the determination of the radiation balance and in the remote sensing of clouds, as basic research, as a contribution to an improved climate modeling, and as a mandatory condition for detecting and monitoring human influences on the cloudy atmosphere.

In climate models the physics of radiative transfer are required for determining heating and cooling rates for the entire climate system. For a long time practical solutions of the radiative transfer equation have been available for plane-parallel atmospheric layers only. Thus, for climate modeling and for remote sensing applications clouds have been and still are idealized by stratiform layers. This may appear as a reasonable simplification for cloud dimensions are much larger along the horizontal than along the vertical direction. However, the spatial scales that are relevant for radiative transfer, i. e. the mean the path lengths between two successive extinction[1] processes,

[1]In the context of this work, the word extinction is ment to summarize scattering and absorption processes.

Figure 1: “Sea of clouds”. Taken from the “Karslruher Wolkenatlas” with kind permission by Bernhard M”uhr.

can be as small as several meters depending on the cloud optical thickness. Since the relationship between radiative and cloud properties is non-linear in most situations, the radiative properties of a homogeneous, i. e. spatially averaged cloud, systematically deviates from the domain averaged radiative properties of a more realistic inhomogeneous cloud. For example, the assumption of plane-parallel clouds leads to a systematic overestimation of the amount of reflected solar radiation (*albedo bias*) (Cahalan et al., 1994).

Clouds are a global phenomenon. Therefore, cloud monitoring requires reliable satellite based remote sensing methods. As for the radiation budget problem this implies the need for a most realistic radiative transfer modeling in order to obtain unbiased relationships between the radiances measured at the satellite radiometer and the state of the cloudy atmosphere that causes these radiances.

Another commonly used simplification in cloud radiative transfer is the general application of Mie-theory, i. e. the assumption of perfectly spherical particles. This assumption is well justified in the case of water clouds. However, already rain drops and in particular ice particles in mixed-phase and cirrus clouds show pronounced deviations from a spherical shape which leads to large errors if the scattering and absorption properties of those particles are approximated by means of Mie-theory. For example, scattering at non-spherical particles is more isotropic compared to that of surface- and volume-equivalent spheres. Thus, the use of Mie-theory applied to non-spherical particles produces an *albedo bias* similar but with opposite sign to the use of homogeneous clouds in case of spatial inhomogeneous cloud fields.

With that the specific goals of my work are focused on considering

1. the non-sphericity of atmospheric particles in single scattering calculations, in particular for cirrus clouds, and

2. the 3d spatial structure of clouds in multiple scattering calculations,

i. e. on the two major geometry effects of cloud micro- and macrophysical properties on the radiative transfer in the cloudy atmosphere.

My cumulative habilitation represents a section of my scientific work over the past seven years that is thematically based on the following five publications.

1. Macke, A. and Mishchenko, M. I., 1996. Applicability of regular particle shapes in light scattering calculations for atmospheric ice particles. *Appl. Opt.*, 35, 4291–4296.

   A systematic test regarding the applicability of idealized ice particle shapes for calculating the single scattering and absorption properties of realistic ice crystals in cirrus clouds.

2. Macke, A., Francis, P. N., McFarquhar, G. M., and Kinne, S., 1998. The role of ice particle shapes and size distributions in the single scattering properties of cirrus clouds. *J. Atmos. Sci*, 55(17), 2874–2883.

   A statistical estimate of the uncertainties in size distribution averaged scattering and absorption properties that are caused by a priori assumptions regarding the size distribution in specific applications.

3. Macke, A., Mishchenko, M. I., and Cairns, B., 1996a. The influence of inclusions on light scattering by large ice particles. *J. Geophys. Res.*, 101, 23,311–23,316.

   The development and application of a new model that accounts for light scattering and absorption at non-spherical inhomogeneous particles by means of combining geometric optics and Monte Carlo radiative transfer methods.

4. Macke, A., Mitchell, D., and von Bremen, L., 1999. Monte Carlo radiative transfer calculations for inhomogeneous mixed phase clouds. *Phys. Chem. Earth (B)*, 24(3), 237–241.

   Realization of a fully 3d solar radiative transfer model where all radiative properties (extinction coefficient, scattering phase function, single scattering albedo) are spatially inhomogeneous.

5. Scheirer, R. and Macke, A., 2001a. On the accuracy of the independent column approximation in calculating the downward fluxes in the UV-A, UV-B and PAR spectral ranges. *J. Geophys. Res.*, 106(D13), 14,301–14,312.

   Evaluation of the error in spectral integrated solar irradiances that are caused by commonly used idealizations in the representation of clouds in radiative transfer calculations.

Except for (Scheirer and Macke, 2001a) all publications have been directed by myself. The co-authors have contributed with helpful discussions(M.I. Mishchenko, B. Cairns), by providing data (P.N. Francis, G.M. McFarquhar, S. Kinne) and results from cloud models (D. Mitchell, L. von Bremen). The work by Scheirer and Macke (2001a) represents a continuation of (Macke et al., 1999) and has been development under my scientific supervision. The following summary lists further first- and co-author publication of mine that are related to the five selected paper.

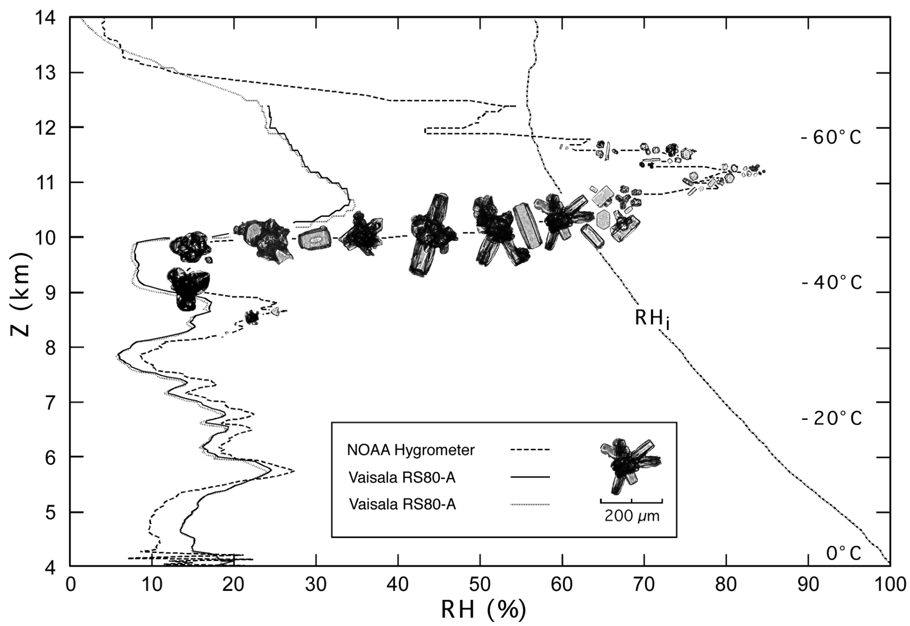

Figure 2: Schematic illustration of the development of ice particle size and shape. Ice particle replicates are plotted along a vertical profile of relative humidity with respect to water. From Miloshevich et al. (2001).

2 Single scattering at ice particles in cirrus clouds

Our understanding of climate processes is considerably hampered by the lack of knowledge regarding the contribution of cirrus clouds to the radiation budget and the feedback mechanisms associated with this cloud type with respect to natural and anthropogenic climate fluctuations (e. g. Liou, 1986). The theoretical description of scattering and absorption properties of atmospheric ice particles is rendered difficult by the strong variability in particle size and shape. However, that knowledge is a necessary condition for the interpretation of remote sensing data and for determining the radiation budget. In general, the optically thin cirrus clouds are associated with a net warming due to the large transmissivity for solar irradiance and the small thermal emission at the cold cloud tops. However, the net effect critically depends on optical thickness and particle size spectra and may respond either positive or negative to changes in our climate (Zhang et al., 1999). Furthermore, the net radiation budget of cirrus clouds is directly affected by the steady increase of emissions from aircrafts resulting in larger global cirrus cloud cover and in a modification of cirrus microphysical properties (indirect aerosol effect).

Figure 2 illustrates the changes in shape and size of atmospheric ice crystals as they grow from micrometer sized "quasi-spheres" to millimeter sized dendrites of hexagonal columns (bullet rosettes) to melting lumps of irregular shaped ice particles. Since the particle sizes vary along three orders of magnitude the averaged scattering and absorption properties also significantly depend on the choice of the size distribution.

2.1 Scattering theory and ice particle models

Atmospheric ice crystals are large compared to the wavelength of the incoming solar radiation which allows to apply the geometric optics method (GOM) to calculate their extinction properties. Here, the intensity and polarization state of a sufficiently large number of incoming rays is traced by simulating the reflection and refraction processes at a predefined particle geometry. By collecting all rays that are refracted out of the particle and by accounting for diffraction at the particles geometrical cross section it is possible to obtain the scattering, polarization, and absorption properties of that particle. In contrast to the Mie-theory, the GOM is applicable to arbitrary particle shapes as long as the smallest dimension of the particle is large compared to the wavelength of the incoming radiation.

From the molecular structure of ice it is to be expected that macroscopic ice crystals have a hexagonal shape. Despite the fact that in-situ measurements in most cases reveal more complex crystal shapes, the first light scattering models based on the GOM have focused on hexagonal columns and plates. (Takano and Liou, 1989, 1995). It was not until a number of discrepancies arose from this approach that led to a change of mind. For example, a comparison between modeled and observationally derived solar radiant flux densities indicated a typical value of 0.7 to 0.75 for the asymmetry parameter[2], whereas hexagonal symmetric crystals have values larger than 0.8 (Stackhouse and Stephens, 1991; Kinne et al., 1992). Furthermore, the observed angular dependency of the reflected and transmitted radiance is much smoother compared to model results based on hexagonal crystals. (Francis, 1995; Brogniez et al., 1995; Gayet et al., 1995).

The "fractal polycrystal" introduced by Macke et al. (1996b) provided asymmetry parameter and radiance fields that fitted significantly better to the observations. This particle type is supposed to represent a scattering geometry that at the same time has crystalline and irregular properties. This geometry corresponds more to an ensemble of differently shaped ice crystals rather than to an observed particle shape. I was involved in a number of theoretical and experimental studies that have included the fractal polycrystal in their investigations (Francis, 1995; Mishchenko et al., 1996; Mitchell et al., 1996; Mitchell and Macke, 1997; Francis et al., 1998; Chepfer et al., 1999; McFarquhar et al., 1999; Zhang et al., 1999; Doutriaux-Boucher et al., 2000; Labonnote et al., 2000, 2001; Zhang et al., 2001; McFarquhar et al., 2001). For the present mentioned are Mishchenko et al. (1996) who layed the basis for applying the fractal polycrystal to the remote sensing algorithm of the International Satellite Cloud Climatology Projects ISCCP, and Mitchell et al. (1996) who developed a parameterization of the solar radiation balance based on this particle type for use in climate models. This parameterization has been integrated into the climate models HadM3 (Hadley Center, UK) and UKMO(UK Meteorological Office), and has led to more consistent calculations of the solar heating rates in the upper troposphere (Kristjansson et al., 1999, 2000).

Since the GOM becomes less valid as the size parameter[3] decreases, its application must be regarded as problematic for the smallest [almost all] ice crystals in the solar [thermal] spectral range. For the first time, Macke et al. (1995) quantified the error of the GOM when applied to non-spherical particles. By comparing results from the GOM and the exact T-matrix method (Mishchenko, 1993) we found that the approximation of the GOM produces smaller errors in case of non-spherical particles than in in case of surface- or volume-equivalent spheres. Thus, non-sphericity comes to meet the GOM! For moderately absorbing particles, the scattering properties are in good agreement for size parameter above 60, the single scattering albedo[4] for size parameter

[2] mean cosine of the scattering angle, measure for the anisotropy of the scattered radiation.
[3] ratio of particle size and wavelength
[4] 1 - absorptivity

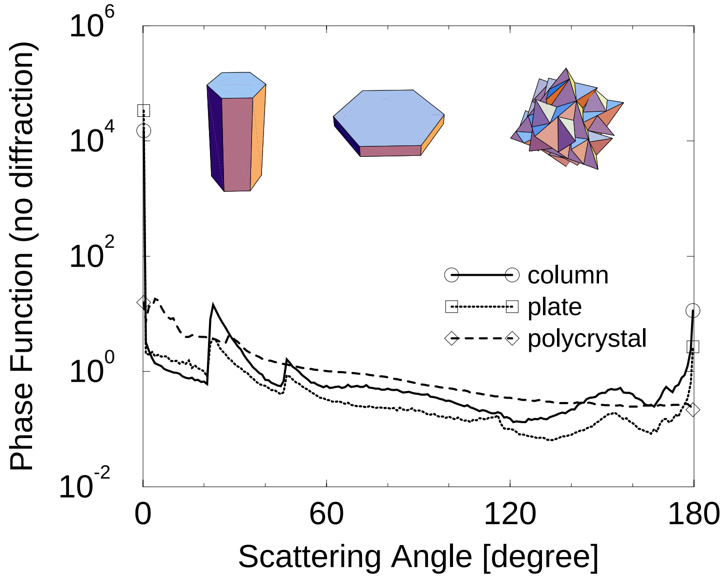

Figure 3: GOM results for the scattering phase function (excluding diffraction) of 3d randomly oriented columns, plates and fractal polycrystals at a wavelength of 0.5 μm. From Macke et al. (1998).

above 10, already. Later, Wielaard et al. (1997) and Mishchenko and Macke (1999) showed that non-absorbing particles reach a satisfying agreement above size parameter of about 120.

For numerical reasons, the T-matrix method is limited to size parameter smaller than 200 (Wielaard et al., 1997). Therefore, our intercomparison studies have shown that a combination of GOM and T-matrix method provides a complete coverage of all particle sizes or wavelengths, respectively.

Since the T-matrix method is limited to symmetrical particle shapes (spheroids, circular cylinder, ...) the findings shown above are justified when applied to those compared to real ice crystals strongly idealized particle geometries . The question therefore arises to what extend these simplifications resemble the scattering and absorption properties of real ice particles. To answer this question, Macke and Mishchenko (1996) have compared the GOM results for the following four particle geometries:

- hexagonal cylinder and fractal polycrystals as the two extremes of realistic ice particles, and
- geometric cross-sectional- and aspect ratio equivalent ellipsoids and circular cylinder as possible particle shapes in the framework of the T-matrix method.

It turns out that the use of those idealized shapes leads to unacceptable large differences in the non-absorbing visible and the moderately absorbing near infrared spectral range. Only at strongly absorbing wavelengths similar results are found for hexagonal and circular cylinders.

In summary, however, it must be concluded that the use of idealized particle shapes does not sufficiently account for the extinction properties of real ice crystals. Therefore, the combination of GOM and T-matrix method is not applicable to simulate the scattering and absorption properties of realistically shaped ice particles over the entire spectral range. The Finite Difference Time Domain Method FDTD provides exact solutions for finite hexagonal cylinder, however, this method is limited to size parameter smaller than 15 - 20 (Yang and Liou, 1995). Therefore, a combination of GOM and FDTD would still leave a gap in the size parameter range from 20 to 100. Until today, there is no theory available that allows for exact solutions for irregular shaped particles.

2.2 The effect of variable cloud microphysical properties

At least for the solar spectral range, the GOM provides a practicable way to solve the scattering problem for the majority of particle sizes. Direct applications of the GOM in radiative transfer calculations require specific choices regarding the particle geometry and the particle size distribution. In order to estimate the statistical errors that may result from those specifications, Macke et al. (1998) have calculated size distribution averaged scattering phase functions and single scattering albedos for a large number of observationally derived ice crystal size distributions. The maximum number of available distributions from US-American and European field experiments have been collected, in order to obtain an optimum coverage of the natural variability of real ice particle spectra.

The crystal geometries that went into the calculations of the averaged properties were hexagonal columns, hexagonal plates, and fractal polycrystals. Fig. 3 shows the scattering phase functions at the visible spectral range of those essentially different particle shapes. The hexagonal particles provide pronounced forward scattering due to transmission through plane-parallel facets, the large backscattering caused by retroreflection at perpendicular facets, as well as the 22°and 46°halos from tranmission through 60°and 90°prisms. Hexagonal plates have larger tranmission maxima and less side- and backscattering compared to columns. The irregular polycrystal is lacking "typical ray paths" and thus shows a much smoother scattering signature.

Figure . 4 shows the probability density distributions of the asymmetry parameter g and the single scattering albedo ω_0 that result from the different particle size spectra. The asymmetry parameter at visible wavelengths is most responsible for the solar energy budget since the solar irradiation is strongest and ice has negligible absorption at these wavelengths. The important result of this work is that the $g(0.5\mu m)$ distribution for the different particle types do not overlap, i. e. that the choice of ice crystal geometry has a stronger influence on the solar radiation budget than the choice of the particle size distribution.

The size of ice crystal affects the scattering and absorption properties by 1) the size dependent aspect ratio of hexagonal crystals (Auer and Veal, 1970) leading to stronger transmission and smaller side- and backscattering at larger sizes, and 2) by the less isotropic diffraction at larger geometrical cross sections. The latter effect is negligible, though, as can be seen from the almost δ-peaked $g(0,5\mu m)$ distribution for the irregular polycrystal whose shape does not change with size.

The moderate absorption at 1.6 μmwavelength adds a further size dependency leading to broadening and partly overlap of the distributions for the different ice particle types. Nevertheless, the latter are still distinguishable as the standard deviation of the individual distributions are smaller than the distance between the modes. Thus, also in the solar near infrared the choice of particle type has a dominant effect compared to the choice of size distribution. The same is true for the absorptivity for columns and plates, as can be seen from the $\omega_0(1.6\mu m)$-distribution. The

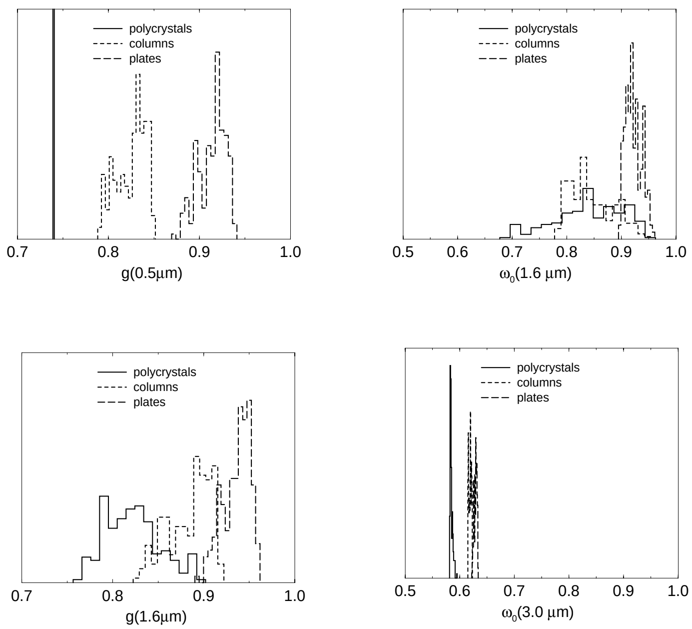

Figure 4: Frequency distributions (arbitrary units) of the asymmetry parameter g at a wavelength of 0.5 μmand 1.6 μm, and of the asymmetry parameter at a wavelength of 1.6 μmand 3.0 μm. From Macke et al. (1998).

more compact shaped irregular polycrystal absorbs radiation more efficiently than its hexagonal counterpart, thus reacting more sensitive to different size distributions and yields the smallest values for the single scattering albedo, which is also confirmed by the distribution at the strongly absorbing spectral region at 3.0 μmwavelength. Here, the absorption is nearly saturated and the variation with size spectra is correspondingly small.

How does the variability in ice particle shape and size affect the solar radiative transfer in cirrus clouds? To answer this question Schlimme and Macke (2001) have calculated the solar broadband cirrus radiation budget by means of a Monte Carlo radiative transfer code for 114 different size distributions from mid-latitude cirrus clouds for hexagonal columns and fractal polycrystals, respectively. Clouds were assumed as homogeneous and plane-parallel to focus on the effect of microphysical properties on the radiative transfer. The resulting radiant flux densities are shown in Fig. 5 as a function of cloud optical thickness. As in the case for the distribution-averaged single scattering, the radiative fluxes differ stronger for different particle shapes than for different size distributions. However, from this results it is possible to quantify the uncertainty in the cirrus solar radiative budget that is caused by uncertainties in the ice crystal size distributions.

For irregular shaped particles the reflectivity varies around 4%, the transmissivity around 2 - 3% and the absorption from 9 to 25% with increasing optical thickness. Hexagonal columns are more sensitive to ice particle size as mentioned above and here reflection varies around 7%, transmission around 1% and absorption around 20 to 6% with increasing optical thickness. The uncertainties are largest for absorption also in absolute numbers ranging from 15 to 20 Wm^{-2} depending on particle type.

Even in the unrealistic case that the ice crystal shape would be well known the uncertainties in the particle size distributions would result in corresponding uncertainties in the solar radiative budget

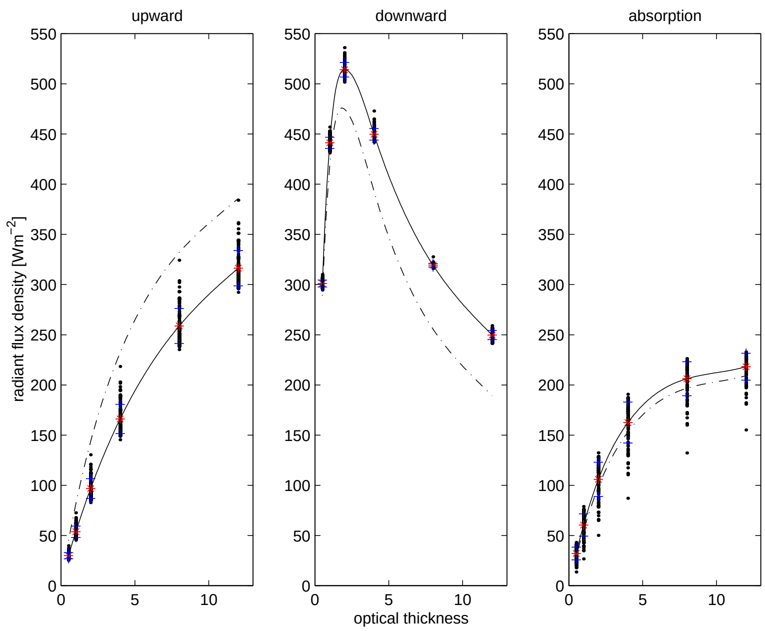

Figure 5: Solar broadband reflected, transmitted and absorbed radiative fluxes for 114 different ice particle size distributions as a function of cloud optical thickness. Solid (dashed) line: mean curve for hexagonal columns (fractal polycrystal). In order to keep perspective only the mean curve is shown for the fractal polycrystal. From Schlimme and Macke (2001).

of this cloud type, that are one order of magnitude larger than the discussed anthropogenically induced radiative forcing.

2.3 Inhomogeneous ice particles

A combination of hexagonal and irregular shaped (fractal polycrystal) ice particles enables a more or less realistic description of the average scattering properties as demonstrated in McFarquhar et al. (1999). However, the contributions from the polycrystals provides an overestimation of absorption, caused by the compact shape of this particle type. Another way of combining hexagonal symmetric and irregular ice crystal properties that bypasses this problem results from the Monte Carlo GOM concept that I have developed (Macke et al., 1996a; Macke, 2000). The idea is to allow for internal multiple scattering events inside a certain "host particle" as illustrated in Fig. 6. This multiple scattering is realized by Monte Carlo processes, i. e. the free path lengths, direction and attenuation of a previously straight light ray are subject to changes depending on the optical thickness and the scattering and absorption properties of internal particles. The scattering and absorption properties of those inclusions are determined beforehand. The following MC-GOM results are based on spherical inclusions. Of course, non-spherical particles can be considered as well, as long as their extinction properties relative to the host medium can be calculated with a suitable light scattering method.

Examples for inclusions in atmospheric ice particles are air bubbles or scavenged aerosol particles. Other inhomogeneities like microscopic breaks or steps act like local scatterers and may be accounted for by means of the Monte Carlo GOM concept as well.

The changes in the scattering properties of hexagonal ice columns with increasing optical thickness

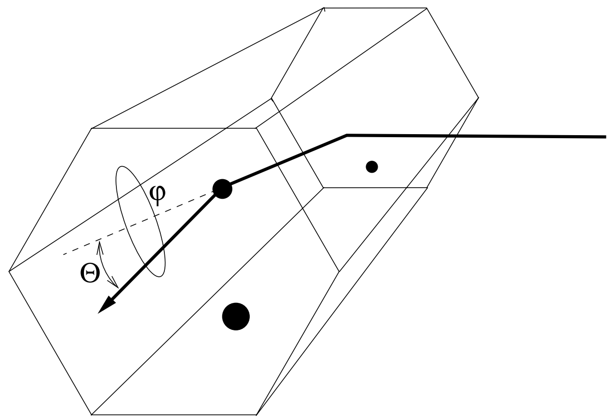

Figure 6: Illustration of the consideration of internal scattering processes inside a hexagonal host particle. An incoming ray is refracted into the particle and is internally scattered at an inclusion around a zenith angle Θ and an azimuth angle φ. From Macke (2000).

of internal conclusions is shown in Fig. 7 for three different types of inclusions: ammonium sulfate, soot, and air bubbles. Ammonium sulfate and soot may origin from aircraft exhausts and industrial emissions. Air bubbles are formed by rapid crystal growth and by spontaneous freezing of supercooled water droplets.

For all three types of inclusions multiple scattering inside the host particle leads to reduction of forward and backscattering, as well as the halo peaks. In the case of the non-absorbing air bubbles and ammonium sulfate particles side scattering increases resulting in a more isotropic total phase function. The contribution from GO light rays to the total scattering phase function is reduced by absorption at the soot inclusions so that the strongly forward scattering diffraction starts to dominate leading to a reduced side scattering.

The concept of the MC-GOM was taken over by other research groups as well and, for example, serves to construct scattering phase functions that fit best to satellite based measurements of solar radiance fields reflected from cirrus clouds (Labonnote et al., 2001). Contrary to the fractal polycrystal, which is supposed to represent highly irregular shaped ice particles, the so derived phase function has no physical basis anymore. However, it provides optimal input for calculating the cloud radiative budget and for the remote sensing of cloud optical thickness.

A number of years will pass before it will become possible to obtain the scattering and absorption properties of atmospheric ice crystals from a direct adaption of the detailed crystal structures to appropriate light scattering theories.

3 Multiple scattering in inhomogeneous clouds

The above discussed ice clouds are often optically thin and the solar radiative properties strongly depend on the single scattering properties of the individual ice crystals. For deep and low level water clouds, the situation is almost reverse with usually large values for the optical thickness and, at least for pure water clouds, with almost constant single scattering properties. Here the transport of the solar radiation through the spatially inhomogeneous cloud structure becomes the dominant physical process.

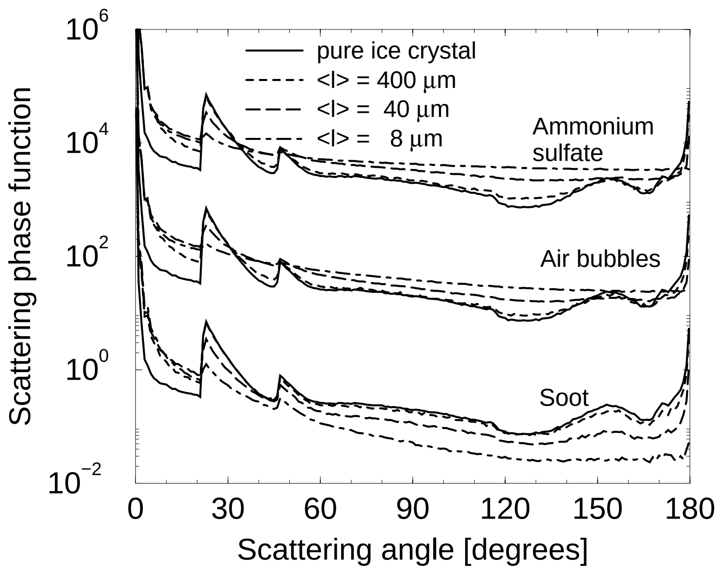

Figure 7: Scattering phase functions of a hexagonal column with spherical inclusions made of ammonium sulfate (multiplied by 10^4), air bubbles (multiplied by 10^2) and soot. From Macke et al. (1996a).

The everyday experience that clouds appear as complex spatial structures to the unaided eye proves the strong relevance of three-dimensional cloud radiative transfer. A few years ago, practical solutions of the radiative transfer equation were restricted to stratiform, i. e. one-dimensional atmospheres. A still up-to.date review of the different methods is given by Hansen and Travis (1974).

Today, modern computer enable almost exact calculations of the 3d radiative transfer by means of the Monte Carlo method (MC-RTM). Here, the scattering and absorption of a photon bundle starting from a certain source (e.g. the sun) are traced until the bundle leaves the system under investigation or until it is completely absorbed. The free path length between two subsequent extinction processes, the change in direction due to a scattering event and absorption are regarded as random processes that follow certain probability density functions determined by the volume extinction coefficient, the scattering phase function and the single scattering albedo (see Marchuk et al. (1980)).

The Spherical Harmonics Discrete Ordinate Method (SHDOM) developed by Evans (1998) directly solves for the radiative transfer equation, also in case of spatial inhomogeneous media. SHDOM is superior to Monte Carlo methods when internal and external radiance fields needs to be calculated. The Monte Carlo approach is faster for calculating domain averaged radiant flux densities. However, the main advantage of the Monte Carlo method lies in the fact that arbitrary intermittent cloud structures and arbitrary anisotropic scattering phase functions are fully accounted for, whereas the numerical expansion of the radiative quantities and the limitation to a finite number of discrete ordinates may lead to inpractical situations for the SHDOM.

3.1 Cloud structures

Until today little is known about the full spatial structure of clouds from an experimental point of view. Measurements by aircraft, cloud radar and spatially high resolved satellite radiometers allow for a one- and two-dimensional probing of clouds. Together with theoretical considerations these measurements have revealed the multispectral nature of the spatial distribution of cloud water (Schertzer and Lovejoy, 1987; Lovejoy and Schertzer, 1990). That means, cloud show inhomogeneous structures on all spatial scales.

Motivated by the fractality of clouds and by the lack of experimentally derived 3d cloud structures 3d radiative transfer calculations have been applied to artifically generated cloud fields first (Breon, 1992; Barker and Davies, 1992; Cahalan et al., 1994; Marshak et al., 1995a,b). These clouds also did not vary in all three directions in space but only considered horizontal variations in cloud optical thickness.

It was not until the availability of small scale 3d atmospheric circulation models with integrated cloud physics that full 3d cloud structures could be accounted for in radiative transfer calculations (Oreopoulus and Barker, 1999; Barker et al., 1999).

The situation becomes more complex in case of mixed phase clouds where the different scattering properties of water droplets, rain drops and ice particles also need to be taken into account. By comparing satellite-based measurements of microwave emission (sensitive to liquid water) and of solar reflectance (sensitive to liquid and ice water) Lin and Rossow (1996) have obtained a global mean ratio of ice to liquid water path of 0.7 for non-precipitating marine clouds.

The recently available mm-cloud-radar also show a large frequency of ice even for low convective mid-level summertime clouds (Markus Quante, 2001; private communications). The existence of ice phase is detected by the strong depolarization at non-spherical melting particles which reveal the transission region between solid and liquid phase.

As an example Fig. 8 shows a time series of radar reflectivity and vertical velocity obtained from the GKSS cloud radar MIRACLE on August 2, 2001. The sudden appearance of large downward fall velocities marks the beginning of precipitation which in turn is a result of coexisting water and ice (Bergeron-Findeisen process) with a predominance of ice particles above the fold.

From all those results it can be expected that a combination of liquid water and ice is more the rule than the exception in atmospheric clouds.

In order to generate 3d mixed phase clouds the 3d non-hydrostatic atmospheric model GESIMA (Eppel et al., 1995) has been applied. The model includes a detailed cloud parameterization developed by Levkov et al. (1992) and modified by Hagedorn (1996). The cloud scheme distinguishes water droplets, rain drops, ice crystals and snow. Fig. 9 shows an example of the evolution of a GESIMA cloud illustrated by the spatial distribution of the volume extinction coefficient at different time steps. The resolution of the model domain is 2 km horizontally and ranges from 100 m at the ground to 1 km at 10 km height along the vertical. With 52 x 52 x 26 grid cells, the whole model domain roughly corresponds to a single grid cell in a global atmospheric circulation model. In order to obtain more or less independent cloud realizations from a certain model run, cloud fields are taken every 10 minutes by an integration time step of 10 seconds. The clouds used in our studies have been calculated by v. Bremen et al. (2001)

3.2 Radiative transfer modeling

The goal of our work is to realize the full 3d radiative transfer which embraces the consideration of 3d structures in volume extinction, scattering and absorption properties. This situation is

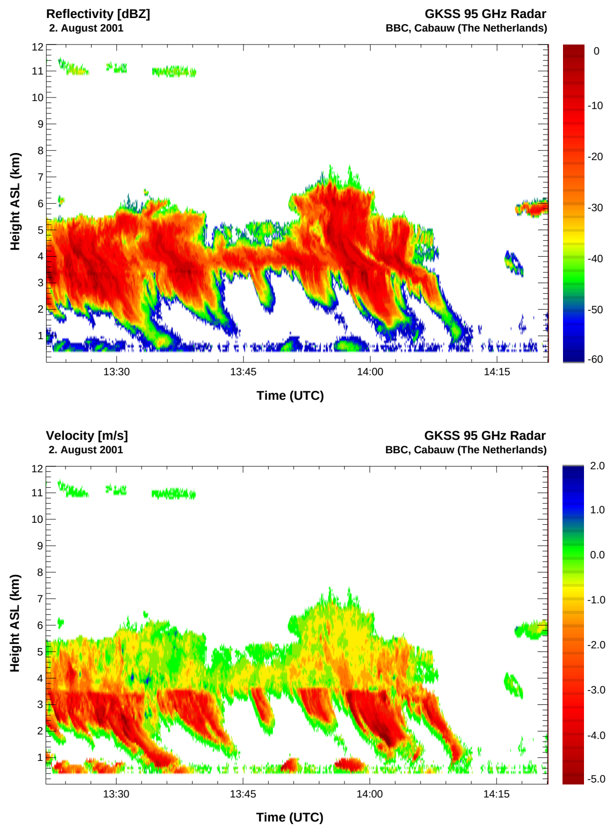

Figure 8: Time series of radar reflectivity (top) and particle fall velocity (bottom) derived from the GKSS cloud radar MIRACLE during the BBC field campaign of the EC project CLIWA-NET.

guaranteed by the different contributions of water droplets, rain, ice and snow in each GESIMA grid cell. Scattering and absorption at the spherical water droplets is calculated by Mie-theory. Macke and Grossklaus (1998) have developed a GOM that accounts for the non-sphericity of rain drops. Snow is regarded as a highly irregular particle type and is thus realized by the fractal polycrystal. Finally, ice particles are taken as hexagonal columns. Each particle type is averaged along a variety of theoretical or observationally derived size distributions so that scattering and absorption properties are available as a function of effective particle radius. This is the case for 14 spectral bands covering the entire solar spectral range. This represents an extensive data base that can be applied to problems in radiative budget calculations and in remote sensing of clouds.

As an example Fig. 10 shows the scattering phase functions of the four different particle types in the visible spectral range as a function of effective particle radius. The building-up of the rainbow peaks with increasing size of the spherical water droplets, the smoothening of the raindrop phase function with increasing non-sphericity, the small changes in the phase functions of the hexagonal particles due to changing aspect ratios are clearly shown. The size-independent shape of the fractal polycrystal does not allow for much changes in the scattering phase function with changing effective radius.

The GESIMA quantities water content and number densities are translated into the radiative relevant quantities volume extinction coefficient and effective radius as described in Macke et al.

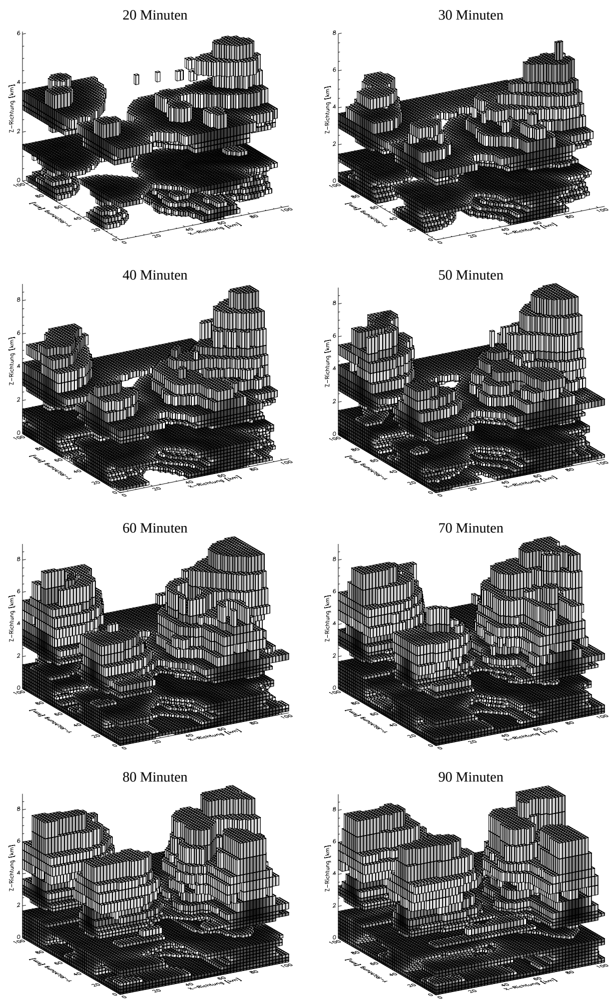

Figure 9: Time series of GESIMA clouds. From Scheirer (2001).

(1999). Here we have investigated the influence of different simplifications in the representation of clouds on the results of radiative transfer calculations in the visible (non-absorbing) spectral range. The following cases have been distinguished.

Case	Description
A-SC	3d inhomogeneous extinction coefficients and scattering properties, open boundaries of the model domain.
A-PB	as case A-SC but with periodic boundary conditions.
B	as case A-SC but with fixed scattering and absorption properties.
C	as case B but with constant extinction properties.
D	as case C but horizontally.
E-W	as case D but with a priori scattering and extinction properties (water droplets with 10 μmeffective radius).
E-I	as case E-W but with an ice particle size distribution with an effective radius of 30 μm.

Case A corresponds to the real radiative transfer problem split into the situation of a single

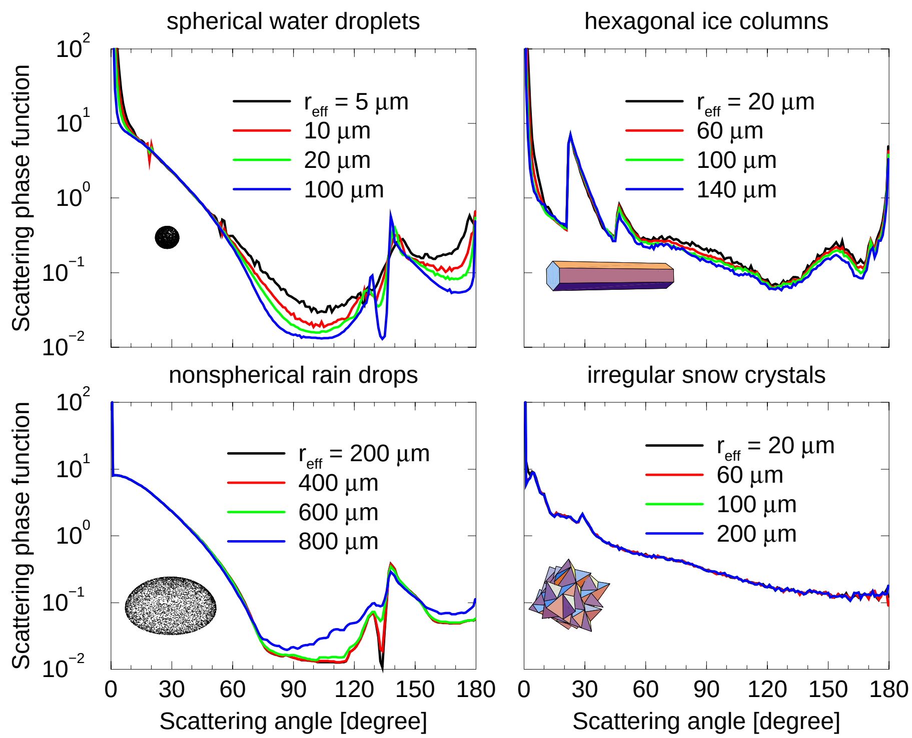

Figure 10: Scattering phase functions of spherical water droplets, oblate raindrops, irregular shaped snow particles and hexagonal ice crystals in the visible spectral range for different effective radii.

cloud (A-SC) and of a cloud field realized by horizontally periodic boundaries (A-PB). Case B represents the commonly used situation to model 3d cloud radiative transfer by varying cloud optical thickness only while keeping the scattering properties fixed. Cases C and D stand for completely homogenized clouds either as an isolated cloud block (C) or as a stratiform cloud (D). The latter corresponds to the classical radiative transfer. However, in D the true mean scattering phase function is used. In praxis, the scattering properties of the cloud particles are not known so that case E must be regarded as the more commonly found situation.

A total of four cloud scenarios have been investigated corresponding to convective summertime clouds (case I), stratiform winter clouds (case II), stratiform summer clouds (case III), and convective late summer clouds (case IV) (Hagedorn, 1996).

Fig. 11 shows the domain averaged albedo as a function of the mean optical depth for the six representations of clouds in radiative transfer. The cases E and D reflect the convex relationship typical for plane parallel homogeneous clouds. Variable mean scattering properties (case D) essentially provide two curves, depending on weather ice or liquid water dominates the radiatively most important upper cloud layers. Accounting for a finite cloud geometry (case C) yields a considerable reduction in albedo because photons are able to penetrate through cloud sides in this representation. This reduction strongly depends on the cloud aspect ratio (ratio of cloud vertical to horizontal dimension) and thus shows a noisy behavior in the albedo curve. A further reduction results from the spatial inhomogeneity of the volume extinction coefficient. The well know reason for this is the above shown non-linear dependency of cloud albedo on optical thickness. As expected, this reduction is strongest for the most inhomogeneous convective clouds.

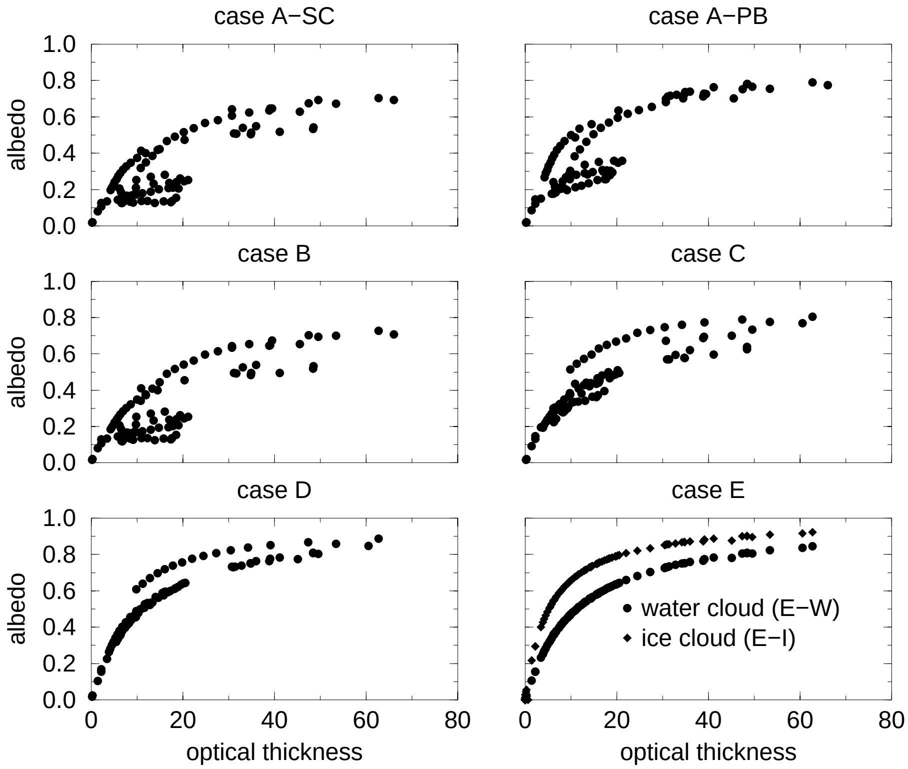

Figure 11: Cloud albedo in the visible (non-absorbing) spectral range as a function of cloud optical thickness for the six cloud representations in radiative transfer. See the text for further explanations. From Macke et al. (1999).

For a fixed optical thickness the cloud aspect ratios are the radiatively most important parameters for isolated clouds. In case of stratified clouds it is the internal cloud structure. The spatial variability of the scattering properties plays a minor role. However, our latest (not yet published) results show that the latter is only the case at the non-absorbing visible spectral region. Spatial inhomogeneous absorption considerably affects the radiative transfer in the solar infrared and even shows up significantly in the domain averaged solar broad band radiative fluxes.

3.3 Error estimate of classical radiative transfer codes

The classical and still widely used method of radiative transfer modeling simplifies the spatial cloud structure to horizontally homogeneous plane parallel (PPHOM) layers. Despite the qualitatively well known errors which result from the PPHOM assumption this method is applied to climate modeling, essentially because of the lack of alternatives that could account for sub-scale radiative transfer (however, see section 3.4!). The so obtained errornous radiant flux densities are roughly tuned to observationally derived radiation budget climatologies.

In order to estimate the PPHOM error Scheirer and Macke (2001a) and Scheirer and Macke (2001b) have compared the results from 3d radiative transfer calculations to those from equivalent 1d calculations. The following PPHOM cases have been distinguished:

1) All cloudy columns are treated as one PPHOM cloud with horizontally averaged cloud properties in each vertical layer (denoted as PPHOM hereafter). This represents the most simple

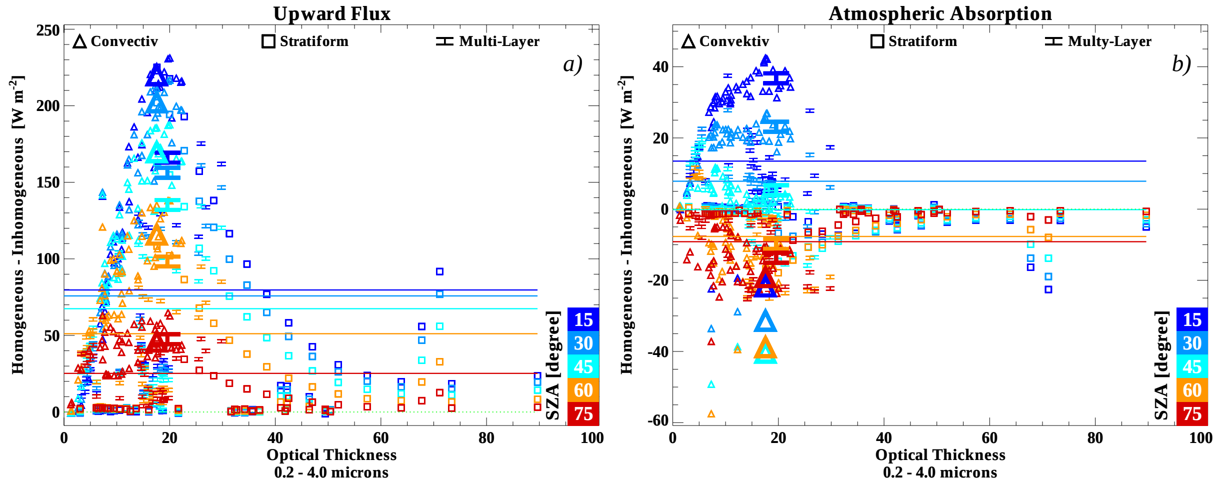

Figure 12: Differences in the solar broadband radiative fluxes between PPHOM and 3d radiative transfer calculations. From Scheirer (2001).

approximation, thus produces the largest errors, and corresponds to the situation where no information on the internal cloud structure is available.

2) Each cloudy column is treated as PPHOM case separately and the results of all columns are averaged (Independent Column Approximation ICA). This corresponds to the optimal solution that makes use of 1d radiative transfer models. However, the ICA requires the full knowledge on the spatial cloud structure within the domain.

A similar study on the errors associated with those idealizations has also been performed by Oreopoulus and Barker (1999) and by Barker et al. (1999). There, 3d radiative transfer is restricted to spatial inhomogeneous volume extinction coefficient whereas our studies additionally account for variations in scattering and absorption properties. Furthermore, these paper provide a qualitative estimation based on a few example clouds whereas a large number of cloud realizations is used here in order to obtain a specific dependency of the errors on cloud optical thickness and cloud type.

Fig. 12 clearly demonstrates that the assumption of homogeneous cloudiness leads to massive overestimations of the solar broadband radiant flux densities up to 230 Wm^{-2}, in particular for high sun elevation and for convective cloud types. For this situation the solar radiation is efficiently transmitted through horizontal cloud gaps. Compared to the 3d results absorption is overestimated [underestimated) by as much as 40 Wm^{-2} for high [low] solar elevations. Averaging over all cloud realizations yields a mean overestimation in reflexion of 70 Wm^{-2} whereas the errors in absorption cancel out by chance.

Fig. 13 shows that the ICA produces much smaller errors as those resulting from assuming completely homogeneous clouds. In fact, the differences compared to the 3d results are close to zero on average. Thus, the use of 1d radiative transfer models is acceptable for domain averaged solar radiative fluxes as long as the models are applied column by column to realistic small scale 3d cloud distributions. These findings confirm the qualitative results by Barker et al. (1999).

The problem remains to parameterize small scale cloud properties in large scale atmospheric models. Furthermore, a noisy climatological value like the solar radiative flux effects the entire system differently than its mean quantity. This is always the case when the solar radiative flux

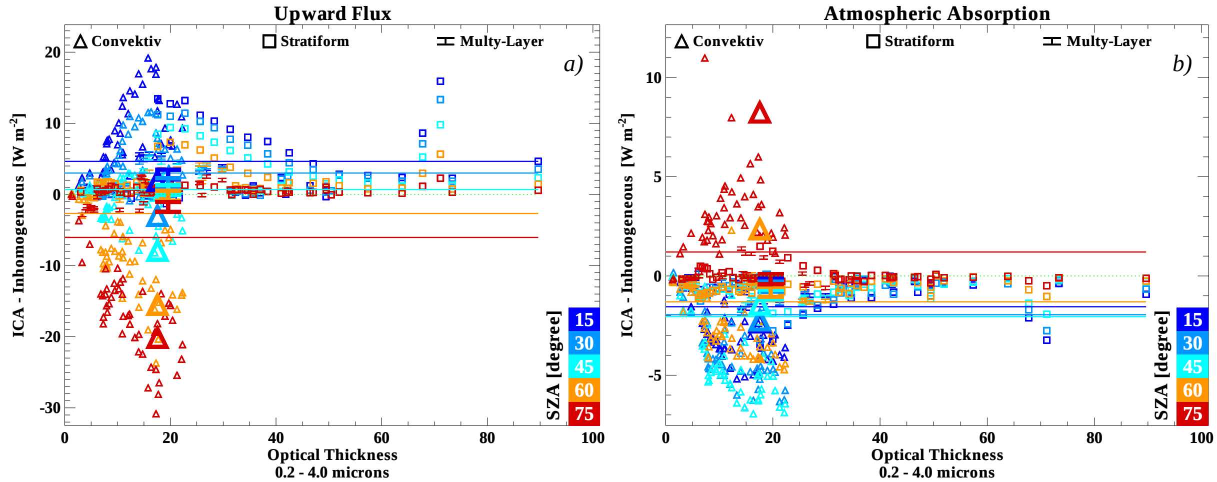

Figure 13: Differences in solar broadband radiative fluxes between ICA and 3d radiative transfer calculations. From Scheirer (2001).

acts in a non-linear way onto the heating rates of the earth/atmosphere system.

3.4 Parameterization of the solar radiant flux densities in large scale atmospheric models

As shown in section 3.3 the assumption of homogeneous clouds leads to inacceptable errors in the radiation fluxes. On the other hand, if the cloud structure is known the ICA appears to be reliable approximation to the domain averaged 3d radiative transfer problem. However, since the the cloud structure is not known in general, we do not have the material at hand to apply it to the reliable tools. The following approach tries to bypass this "lack of material" by simply correlating the domain average radiative fluxes with the domain average cloud properties for a large number of 3d cloud realizations (Schewski et al., 2001; Schewski, 2001). The quality of this correlation is a measure of the functional dependency between domain average cloud and radiative properties. Real applications of this parameterization than would also require to add some noise onto this functional dependency to account for realistic fluctuations in the interactions between clouds and the other components of the climate system.

Our parameterization is based on 168 cloud fields generated with the mesoscale model GESIMA. For each cloud realization the domain average solar broad band reflection R at the top of the model domain, the absorption A within the domain, as well as direct T_{dir}, diffuse T_{dif} and total transmission T_{tot} transmission at the bottom of the domain have been calculated by means of a 3d Monte Carlo radiative transfer model. The results are summarized into a "radiation vector"

$$\underline{\mathbf{R}}_i = [R, A, T_{tot}, T_{dif}, T_{dir}]_i, \quad i = 1, 168 \tag{1}$$

Similarly, the domain average state of the cloudy atmosphere is defined by a "cloud vector"

$$\underline{\mathbf{C}}_i = [LWP, IWP, RWP, SWP, N, H, T, Z_{bot}]_i, \quad i = 1, 168 \tag{2}$$

R	A	T_{tot}	T_{dif}	T_{dir}
LWP 0.802	H 0.846	LWP 0.927	N 0.648	N 0.941
LWP, N 0.929	H, T 0.899	LWP, SWP 0.957	LWP, N 0.945	LWP, N 0.979
LWP, RWP, N 0.957	IWP, H, T 0.924	LWP, RWP, SWP 0.971	LWP, N, CH 0.968	LWP, SWP, N 0.982

Table 1: Optimal cloud parameter for one-, two- and three-parameter regressions according to eq. (3). The resulting correlation coefficients between original and parameterized fluxes are shown as well. From Schewski (2001).

where LWP, IWP, RWP, SWP denote the water paths for cloud liquid water, ice, rain and snow, N the cloud cover, CH the geometrical cloud height, T^{CT} the cloud top temperature and Z_{Bot} the cloud bottom height.

Of course, it is possible to construct more domain average cloud parameters like water content, cloud cover and temperature in each vertical layer. However, this would require a similar resolution of the radiation vector $\underline{\mathbf{R}}_i$ and the 168 cloud scenes used here would hardly suffice to obtain a meaningful correlation. Still, there is large potential in this kind of correlation approach provided that a sufficiently large number of cloud realizations are at hand. In this case a neural network would be the method of choice to obtain the optimum nonlinear relation $\underline{\mathbf{F}}_i = f(\underline{\mathbf{C}}_i)$ between average cloud and average radiation properties. Due to the limited number of clouds used in this study, a simple non-linear regression of the form

$$F_j = a_j + \sum_{k=1}^{N_C} b_{jk} C_k^{\frac{1}{2}} + c_{jk} C_k + d_{jk} C_j^2 \tag{3}$$

has been performed, where the $a_i, b_{ij}, c_{ij}, d_{ij}$ are the regression coefficients and N_C the number of cloud parameters.

The regression has been performed for a maximum of three cloud parameters, i. e. 10 regression coefficients. A larger number would just map the situation of the 168 clouds used in the regression to the expense of generality. With a simple trial and error approach those cloud parameters have been selected for each radiative flux that provide the best regression. The results divided into one-, two- and three-parameter regressions are shown in Table 1.

The domain averaged cloud parameter that strongest determines the amount of reflected solar radiation is cloud liquid water, followed by cloud cover and rain water path. For a cloudy region, the amount of cloud water basically determines the amount of radiation that is reflected back to space. The separation into cloudy and cloud free areas considerably improves the regression. Rain water path may point to clouds with strong convection and thus pronounced inhomogeneous cloud structure that reduces the reflectivities compared to non-precipitating clouds with the same amount of liquid water.

The absorption is best correlated with geometrical cloud height with further improvements resulting from taking cloud top temperature and ice water path into account. The strong sensitivity to cloud height suggests that absorption at the cloud particles happens throughout the vertical extension of the cloud. This may be due to the 3d nature of clouds that allows the incoming photons to penetrate through cloud sides into deeper regions of the cloudy body where they get more efficiently absorbed compared to the 1d situation where a large portion of radiation is reflected from the upper cloud regions and thus cannot participate to absorption processes in the lower cloud parts. Cloud top temperature indicates the presence of ice at cloud top, which modifies the total absorption by reflecting more light from the cloud system than liquid water with the same water path. For the same reasons, ice water path provides a further improvement in the parameterization of solar broadband absorption.

The presence of clouds is a necessary condition for diffuse transmission and usually reduces the amount of direct transmitted light close to zero. Therefore, cloud cover shows up as the dominant domain averaged cloud property for those two radiative quantities. Liquid water path adds information about the amount of radiation that is diffusely or directly transmitted through the cloud field. Cloud height is the third best parameter in the parameterization for diffuse transmission, whereas it is snow water for the direct transmission.

We do not intent to generalize the ranking of cloud parameters discussed above. It may well be, that some of the correlations are an artefact of the special choice of cloud fields used in the present study. However, the remarkable finding is that two- and three-parameter regressions already produce surprisingly robust links between the domain averaged cloud and radiation properties despite the highly irregular structure of the clouds. Obviously, part of the information of the 3d cloud structure is hidden in the domain averaged cloud properties and the detailed knowledge of the 3d cloud structure is not required for the parameterization.

4 Summary and Conclusion

The work summarized in this thesis aims on the most realistic modeling of solar cloud radiative transfer to obtain the solar radiation budget of the cloudy atmosphere and to quantitatively estimate the errors associated with simplified treatments of clouds in classical radiative transfer models. The focus is on the geometrical aspect, i. e. on shape, size and spatial distribution of atmospheric hydrometeors. While for fixed optical thickness the radiation properties of cirrus clouds are mostly affected by size and shape of the ice particles, the macrophysical fluctuations are challenging the radiative transfer for deep and low level clouds.

The single scattering models that I have developed based on the Geometric Optics approximation allow for light scattering calculations for arbitrary shaped inhomogeneous large particles. These models have been approved in cirrus cloud radiative transfer modeling and serve for a wide range of applications. Present instrumental techniques and single scattering theories do not allow to obtain scattering and absorption properties of ice particles on the basis of observationally derived crystal geometries. However, the models shown here allow to determine realistic scattering properties from minimizing observed and simulated radiance fields. This will become a promising application with regard to future satellite missions. In particular the classification of the so obtained scattering properties into certain climatological domains will provide helpful information for modeling the radiation budget and for the remote sensing of cirrus cloud optical thickness.

However, uncertainties with regard to the radiative properties will always remain and thus need to be quantified as we have done in case of the effect of the generaly unknown size distributions on the solar radiation budget of cirrus clouds.

Based on my single scattering models for non-spherical hydrometeors (ice and snow crystals, raindrops) it was a consistent step towards investigating the full 3d multiple scattering problem, i. e. towards considering 3d inhomogeneous distributions of optical thickness, scattering and absorption properties as it is to be expected in mixed phase clouds. To this end Monte Carlo radiative transfer models have been developed that calculate domain averaged spectral broadband solar radiative fluxes at predefined cloud structures with reasonable computational expense. The GESIMA clouds used here are by no means representive for the global distribution of possible atmospheric cloud fields. However, they represent a cloud subset large enough to draw some general conclusions.

The non-absorbing visible spectral range is not very sensitive to spatially inhomogeneous scattering properties, whereas inhomogeneous absorption strengths strongly determine the solar infrared which still show up in the solar broadband fluxes (not shown). As shown in previous work on pure water clouds, the ICA provides a reasonable approximation to the 3d radiative transfer problem in case of domain averaged radiative quantities for the more complex mixed phase clouds. This renders it possible to continue using classical 1d radiative transfer codes in climate models of information of the sub-scale cloud distribution is at hand. However, as we could show, it is possible to fit domain average radiative quantities to domain average cloud properties with acceptable accuracy. This opens a door to a more statistically based parameterization of cloud radiative fluxes based on a considerably larger and more representative collection of 3d cloud realizations.

After all, the numerical findings summarized here need to be verified both qualitatively and quantitatively against observations. Despite the difficulties in obtaining the instantaneous 3d cloud field and the domain average radiative quantities at the same time, future techniques based on combinations of active and passive cloud remote sensing (Löhnert et al., 2001), as well as the combination of ground based and satellite based cloud remote sensing (van Lammeren et al., 2000) will unfold the relationship between cloud and radiative properties at least for some exemplary cases. This will provide the touchstones for the modeling of cloud physics and cloud radiative transfer and will lead to a stronger collaboration between the two research areas.

References

Auer, A. H. and D. L. Veal, 1970: The dimensions of ice crystals in natural clouds. *J. Atmos. Sci*, **27**, 919–926.

Barker, H., G. Stephens, and Q. Fu, 1999: The sensitivity of domain-averaged solar fluxes to assumptions about cloud geometry. *Q. J. R. Meteorol. Soc.*, **125**, 2127–2152.

Barker, H. W. and J. A. Davies, 1992: Solar radiative fluxes for stochastic, scale-invariant broken cloud fields. *J. Atmos. Sci*, **49**, 1115– 1126.

Breon, F.-M., 1992: Reflectance of broken cloud fields: Simulation and parameterization. *J. Atmos. Sci*, **49**, 1221– 1232.

Brogniez, G., J. Buriez, V. Giraud, F. Parol, and C. Vanbauce, 1995: Determination of effective emittance and a radiatively equivalent microphysical model of cirrus from ground-based and satellite observations during the International Cirrus Experiment: The 18 October case study. *Mon. Wea. Rev.*, **123**, 1025–1036.

Cahalan, R. F., W. Ridgway, W. J. Wiacombe, T. L. Bell, and J. B. Snider, 1994: The albedo of fractal stratocumulus clouds. *J. Atmos. Sci*, **51**(16), 2434–2455.

Cairns, B., A. Lacis, and B. Carlson, 2000: Absorption within inhomogeneous clouds and its parameterization in general circulation models. *J. Atmos. Sci*, **57**, 700–714.

Cess, R. and co authors, 1995: Absorption of solar radiation by clouds - Observations versus models. *Science*, **267**, 496–499.

Chepfer, H., G. Brogniez, L. Sauvage, P. Flamant, V. Trouillet, and J. Pelon, 1999: Remote sensing of cirrus radiative parameters during EUCREX'94. Case study of 17 April 1994. part II: Microphysical models. *Mon. Wea. Rev.*, **127**, 504–518.

Doutriaux-Boucher, M., J.-C. Buriez, G. Brogniez, L. Labonnote, and A. Baran, 2000: Sensitivity of retrieved POLDER directional cloud optical thickness to various ice particle models. *Geophys. Res. Lett.*, **27**(1), 109–112.

Eppel, D. P., H. Kapitza, M. Clausen, D. Jacob, W. Koch, W. Levkov, H.-T. Mengelkamp, and N. Werrmann, 1995: The non-hydrostatic mesoscale model GESIMA. Part II: Parameterizations and applications. *Contr. Atmos. Phys.*, **68**, 15–41.

Evans, K., 1998: The spherical harmonics discrete ordinate method for threedimensional atmospheric radiative transfer. *J. Atmos. Sci*, **55**, 429–446.

Francis, P., P. Hignett, and A. Macke, 1998: The retrieval of cirrus cloud properties from aircraft multi-spectral reflectance measurements during EUCREX'93. *Q. J. R. Meteorol. Soc.*, **124**, 1273–129.

Francis, P. N., 1995: Some aircraft observations of the scattering properties of ice crystals. *J. Atmos. Sci*, **52**, 1142–1154.

Fritz, S. and T. MacDonald, 1951: Measurements of absorption by clouds. *Bull. Amer. Meteor. Soc.*, **32**, 205–209.

Gayet, J.-F., O. Crepel, and J.-F. Fournol, 1995: A new polar nephelometer for in situ measurements of microphysical and optical properties of clouds. In: *Proceedings of the AMS Conference on Cloud Physics, Dallas, Texas, January 15-20, 1995*, pp. 26–30.

Hagedorn, R., 1996: *Hydrologiebilanz im Geesthachter Simulationsmodel der Atmosphäre (GESIMA) als Test der mikrophysikalischen Parametrisierung*. Master's thesis, Mathematisch-Naturwissenschaftliche Fakultät der Christian-Albrecht-Universität zu Kiel.

Hansen, J. E. and L. D. Travis, 1974: Light scattering in planetary atmospheres. *Space Sci. Rev.*, **16**, 527–610.

Kinne, S., T. A. Ackermann, A. J. Heymsfield, F. P. J. Valero, K. Sassen, and J. Spinhirne, 1992: Cirrus microphysics and radiative transfer: Cloud field study on 28 October 1991. *Mon. Wea. Rev.*, **120**, 661–684.

Kristjansson, J., J. Edwards, and D. Mitchell, 1999: A new parameterization scheme for the optical properties of ice crystals for use in general circulation models of the atmosphere. *Phys. Chem. Earth (B)*, **24**, 231–236.

Kristjansson, J., J. Edwards, and D. Mitchell, 2000: Impact of a new scheme for optical properties of ice crystals on climates of two gcms. *J. Geophys. Res.*, **105**, 10063–10079.

Labonnote, L., G. Brogniez, J. Buriez, M. Doutriaux-Bouchert, J. Gayet, and A. Macke, 2001: Polarized light scattering by inhomogeneous hexagonal monocrystals. validation with ADEOS-POLDER measurements. *J. Geophys. Res.*, **106**(D11), 12,139–12,153.

Labonnote, L., G. Brogniez, M. Doutriaux-Boucher, J.-C. Buriez, J.-F. Gayet, and H. Chepfer, 2000: Modeling of light scattering in cirrus clouds with inhomogeneous hexagonal monocrystals. Comparison with in-situ and ADEOS-POLDER measurements. *Geophys. Res. Lett.*, **27**(1), 113–116.

Levkov, L., B. Rockel, H. Kapitza, and E. Raschke, 1992: 3d mesoscale numerical studies of cirrus and stratus clouds by their time and space evolution. *Contr. Atmos. Phys.*, **65**, 35–58.

Lin, B. and W. B. Rossow, 1996: Seasonal variation of liquid and ice water path in nonprecipitating clouds over oceans. *J. Climate*, **9**, 2890–2902.

Liou, K.-N., 1986: Influence of cirrus clouds on weather and climate processes: A global perspective. *Mon. Wea. Rev.*, **114**, 1167–1199.

Löhnert, U., S. Crewell, A. Macke, and C. Simmer, 2001: Profiling cloud liquid water by combining active and passive microwave measurements with cloud model statistics. *J. Atmos. Oceanic Technol.*, **18**(8), 1354–1366.

Lovejoy, S. and D. Schertzer, 1990: Multifractals, universality classes and satellite and radar measurements of cloud and rain fields. *J. Geophys. Res.*, **95**(D3), 2021–2034.

Macke, A., 2000: Monte Carlo calculations of light scattering by large particles with multiple internal inclusions. In: M. I. Mishchenko, J. W. Hovenier, and L. Travis, eds., *Light scattering by nonspherical particles*, chapter 10, pp. 309–322. Academic Press.

Macke, A., P. N. Francis, G. M. McFarquhar, and S. Kinne, 1998: The role of ice particle shapes and size distributions in the single scattering properties of cirrus clouds. *J. Atmos. Sci*, **55**(17), 2874–2883.

Macke, A. and M. Grossklaus, 1998: Light scattering by nonspherical raindrops: implications for lidar remote sensing of rainrates. *J. Quant. Spectros. Radiat. Transfer*, **60**(3), 355–363.

Macke, A., M. I. Michshenko, K. Miunonen, and B. E. Carlson, 1995: Scattering of light by large nonspherical particles: ray tracing approximation versus T-matrix method. *Optics Letters*, **20**, 1934–1936.

Macke, A. and M. I. Mishchenko, 1996: Applicability of regular particle shapes in light scattering calculations for atmospheric ice particles. *Appl. Opt.*, **35**, 4291–4296.

Macke, A., M. I. Mishchenko, and B. Cairns, 1996a: The influence of inclusions on light scattering by large ice particles. *J. Geophys. Res.*, **101**, 23,311–23,316.

Macke, A., D. Mitchell, and L. von Bremen, 1999: Monte carlo radiative transfer calculations for inhomogeneous mixed phase clouds. *Phys. Chem. Earth (B)*, **24**(3), 237–241.

Macke, A., J. Müller, and E. Raschke, 1996b: Single scattering properties of atmospheric ice crystals. *J. Atmos. Sci*, **53**, 2813–2825.

Marchuk, G. I., G. A. Mikhailov, R. D. Nazareliev, R. A. Darbinjan, B. A. Kargin, and E. B. S., 1980: *The Monte Carlo Methods in Atmospheric Optics*. Springer-Verlag.

Marshak, A., D. A., W. Wiscombe, and R. Cahalan, 1995a: Radiative smoothing in fractal clouds. *J. Geophys. Res.*, **100**, 26247–26261.

Marshak, A., A. amd Davis, W. Wiscombe, and G. Titov, 1995b: The verisimilitude of the Independent Pixel Approximation used in cloud remote sensing. *Remote Sens. Environ.*, **52**, 71–78.

McFarquhar, G., P. Yang, A. Macke, and J. Baran, 2001: A new parameterization of single-scattering radiative properties for tropical ice clouds using observed ice crystal size and shape distributions. *JC*, **xx**, xx–xx. Eingereicht.

McFarquhar, G. M., A. J. Heymsfield, A. Macke, J. Iaquinta, and M. Aulenbach, 1999: Use of observed ice crystal sizes and shapes to calculate mean-scattering properties and multispectral radiances: CEPEX April 4, 1993, case study. *J. Geophys. Res.*, **104**(D24), 31,763–31,779.

Miloshevich, L., H. Voemel, A. Paukkunen, A. Heymsfield, and S. Oltmann, 2001: Characterization and correction of relative humidity measurements from Vaisala RS80-A radiosondes at cold temperatures. *JAOT*, **18**, 135–156.

Mishchenko, M. I., 1993: Light scattering by size-shape distribution of randomly oriented axially symmetric particles of a size comparable to a wavelength. *Appl. Opt.*, **32**, 4652–4666.

Mishchenko, M. I. and A. Macke, 1999: How big should ice crystals be to produce haloes. *Appl. Opt.*, **38**(9), 1626–1629.

Mishchenko, M. I., W. Rossow, A. Macke, and A. Lacis, 1996: Sensitivity of cirrus cloud albedo, bidirectional reflectance and optical thickness retreival accuracy to ice particle shape. *J. Geophys. Res.*, **101**, 16973–16985.

Mitchell, D. and A. Macke, 1997: A new treatment of cirrus cloud radiative properties. In: W. Smith and K. Stamnes, eds., *IRS'96: Current Problems in Atmospheric Radiation*, pp. 163–166. A. Deepak Publishing, Hampton, Virginia.

Mitchell, D., A. Macke, and Y. Liu, 1996: Modelling cirrus clouds. part II: Treatment of radiative properties. *J. Atmos. Sci*, **53**, 2967–2988.

Oreopoulus, L. and H. Barker, 1999: Accounting for subgrid-scale cloud variability in a multi-layer 1d solar radiative transfer algorithm. *Q. J. R. Meteorol. Soc.*, **125**, 301–330.

Ramanathan, V., R. D. Cess, E. F. Harrison, P. Minnis, B. R. Barkstrom, E. Ahmad, and D. Hartmann, 1989: Cloud radiative forcing and climate: Results from the earth radiation budget experiment. *Science*, **243**, 57–63.

Ramanathan, V. and co authors, 1995: Warm pool heat budget and shortwave cloud forcing. *Science*, **267**, 499–503.

Rossow, W. B., 1993: *Satellite Observations of radiation and clouds to diagnose energy exchanges in the climate: Part I*, volume 5 of *I: Global Environmental Change*, chapter 5, pp. 123–141. Springer-Verlag Berlin Heidelberg.

Scheirer, R., 2001: *Solarer Strahlungstransport in der inhomogenen Atmosphäre*. Ph.D. thesis, Berichte aus dem Institut für Meereskunde an der Christian-Albrecht-Universität Kiel, Nr. 322.

Scheirer, R. and A. Macke, 2001a: On the accuracy of the independent column approximation in calculating the downward fluxes in the UV-A, UV-B and PAR spectral ranges. *J. Geophys. Res.*, **106**(D13), 14,301–14,312.

Scheirer, R. and A. Macke, 2001b: On the accuracy of the independent pixel approximation in 3d radiative transfer. In: W. L. Smith and Y. M. Timofeyev, eds., *IRS 2000: Current Problems in Atmospheric Radiation*, pp. 229–232. A. Deepak Publishing, Hampton, Virginia.

Schertzer, D. and S. Lovejoy, 1987: Physically based rain and cloud modeling by anisotropic, multiplicative turbulent cascades. *J. Geophys. Res.*, **92**, 9692–9714.

Schewski, M., 2001: *Einfluss dreidimensionaler Bewölkung auf den breitbandigen solaren Strahlungstransport*. Master's thesis, Mathematisch-Naturwissenschaftliche Fakultät der Christian-Albrecht-Universität zu Kiel, Institut für Meereskunde, Kiel.

Schewski, M., A. Macke, R. Scheirer, and T. Jung, 2001: A statistically based parameterisation of shortwave cloud radiative fluxes for inhomogeneous mixed-phase clouds. In: W. L. Smith and Y. M. Timofeyev, eds., *IRS'2000: Current Problems in Atmospheric Radiation*, pp. 249–252. A. Deepak Publishing, Hampton, Virginia.

Schlimme, I. and A. Macke, 2001: Der Einfluss von Kristallform- und Grössenverteilungen auf die solaren Strahlungsfelder von Cirruswolken. In: *Meteorologentagung Wien, 18. - 22. 9., 2001*, number 27/Publ. Nr. 399.

Stackhouse, P. W. J. and G. L. Stephens, 1991: A theoretical and observational study of the radiative properties of cirrus: Results from FIRE 1986. *J. Atmos. Sci*, **48**, 2044–2059.

Stephens, G. and S.-C. Tsay, 1990: On the cloud absorption anomaly. *Q. J. R. Meteorol. Soc.*, **116**, 671–704.

Takano, Y. and K. N. Liou, 1989: Solar radiative transfer in cirrus clouds, part I: Single-scattering and optical properties of hexagonal ice crystals. *J. Atmos. Sci*, **46**, 3–18.

Takano, Y. and K. N. Liou, 1995: Radiative transfer in cirrus clouds. Part III: Light scattering by irregular ice crystals. *J. Atmos. Sci*, **52**, 818–837.

v. Bremen, L., E. Ruprecht, and A. Macke, 2001: Errors in liquid water path retrieval arising from cloud inhomogeneities: The beam-filling effect. *Meteorol. Z.*, **xx**(xx), xx–xx. Accepted.

van Lammeren, A., J. Feijt, A. ad Konings, E. van Mejgaard, and A. van Ulden, 2000: Combination of ground-based and satellite cloud observations on a routine basis. *Meteorol. Z.*, **9**(2), 125–134.

Wielaard, D. J., M. I. Mishchenko, A. Macke, and B. E. Carlson, 1997: Improved T-matrix computations for large, nonabsorbing and weakly absorbing nonspherical particles and comparison with geometric optics approximation. *Appl. Opt.*, **36**, 4305–4313.

Wielicki, B. A., R. D. Cess, M. D. King, D. A. Randall, and E. F. Harrison, 1995: Mission to planet Earth: Role of clouds and radiation in climate. *Bull. Amer. Meteor. Soc.*, **76**(11), 2125–2153.

Yang, P. and K. N. Liou, 1995: Light scattering by hexagonal ice crystals: comparison of finite difference time domain and geometric optic models. *J. Opt. Soc. Am. A*, **12**, 162–176.

Zhang, Y., Z. Li, and A. Macke, 2001: Retrieval of surface solar radiation budget under ice cloudy sky: Uncertainty analysis and parameterization. *J. Atmos. Sci*, **xx**, xx–xx. Eingereicht.

Zhang, Y., A. Macke, and F. Albers, 1999: Effect of crystal size spectrum and crystal shape on stratiform cirrus radiative forcing. *Atmos. Research*, **52**, 59–75.